2011-10-01

A brain-derived MeCP2 complex supports a role for MeCP2 in RNA processing

Steven W. Long
University of Illinois at Urbana-Champaign

Et al.

Biosci. Rep. (2011) / **31** / 333–343 (Printed in Great Britain) / doi 10.1042/BSR20100124

online data

Original Paper

Bioscience Reports

A brain-derived MeCP2 complex supports a role for MeCP2 in RNA processing

Steven W. LONG*, Jenny Y. Y. OOI*, Peter M. YAU*† and Peter L. JONES*‡[1]

*Department of Cell and Developmental Biology, University of Illinois at Urbana-Champaign, B107 Chemical and Life Sciences Laboratory, 601 S. Goodwin Ave., Urbana, IL 61801, U.S.A., †The Carver Biotechnology Center, University of Illinois at Urbana-Champaign, Urbana, IL 61801, U.S.A., and ‡The Boston Biomedical Research Institute, 64 Grove St, Watertown, MA 02472, U.S.A.

Synopsis

Mutations in *MECP2* (methyl-CpG-binding protein 2) are linked to the severe postnatal neurodevelopmental disorder RTT (Rett syndrome). MeCP2 was originally characterized as a transcriptional repressor that preferentially bound methylated DNA; however, recent results indicate MeCP2 is a multifunctional protein. MeCP2 binding is now associated with certain expressed genes and involved in nuclear organization as well, indicating that its gene regulatory function is context-dependent. In addition, MeCP2 is proposed to regulate mRNA splicing and a mouse model for RTT shows aberrant mRNA splicing. To further understand MeCP2 and potential roles in RTT pathogenesis, we have employed a biochemical approach to identify the MeCP2 protein complexes present in the mammalian brain. We show that MeCP2 exists in at least four biochemically distinct pools in the brain and characterize one novel brain-derived MeCP2 complex that contains the splicing factor Prpf3 (pre-mRNA processing factor 3). MeCP2 directly interacts with Prpf3 *in vitro* and *in vivo* and many *MECP2* RTT truncations disrupt the MeCP2–Prpf3 complex. In addition, MeCP2 and Prpf3 associate *in vivo* with mRNAs from genes known to be expressed when their promoters are associated with MeCP2. These results support a role for MeCP2 in mRNA biogenesis and suggest an additional mechanism for RTT pathophysiology.

Key words: methyl CpG-binding domain (MBD), methyl-CpG-binding protein 2 (MeCP2), pre-mRNA processing factor 3 (Prpf3), Rett syndrome, RNA

INTRODUCTION

MeCP2 (methyl-CpG-binding protein 2) was originally identified by its ability to preferentially bind double-stranded DNA containing symmetrically methylated CpG dinucleotides and is the founding member of the MBD (methyl-CpG-binding domain) family of proteins [1,2]. The first biological role for MeCP2 was illustrated by showing that the protein interacts with methylated DNA *in vivo* and could repress transcription by association with a transcriptional co-repressor complex containing Sin3A and HDAC (histone deacetylase) [3–5]. In 1999, a genetic analysis identified mutations in *MECP2* as causal for RTT (Rett syndrome), providing the first direct link between an epigenetic regulator and a human disease [6]. RTT is a severe postnatal neurodevelopmental disorder and one of the most common causes of mental retardation in females [7]. First described in 1966 by Andreas Rett [8], RTT is characterized by a period of apparently normal development from birth to 6–18 months followed by a regression of obtained language and motor skills [7]. RTT patients usually exhibit a deceleration of head growth, respiratory dysfunction, scoliosis, cognitive impairment, seizures and social withdrawal [8,9]. In addition to RTT, numerous *MECP2* mutations have now been linked to a variety of additional disorders, including autism, Angelman syndrome, learning disabilities and mental retardation syndromes [7,10–14].

MeCP2 has been reported to associate with myriad protein partners, including Sin3A [3,5], c-REST and Suv39h1 [15], c-Ski and N-CoR (nuclear receptor co-repressor) [16], Brm [17] and HP1 [18], all supporting a model of MeCP2 interacting with or being a stable component of transcriptional co-repressor complexes, resulting in targeted transcriptional repression of methylated DNA through modification of the chromatin state or chromatin-associated proteins. However, the biological relevance and implications towards RTT for these numerous documented MeCP2 interactions is not clear due in part to the particular

Abbreviations used: Cdk10, cyclin-dependent kinase 10; ChIP, chromatin immunoprecipitation; co-IP, co-immunoprecipitation; CV, column volume; DTT, dithiothreitol; GST, glutathione transferase; HA, haemagglutinin; IP, immunoprecipitation; MeCP2, methyl-CpG-binding protein 2; MBD, methyl-CpG-binding domain; MS/MS, tandem MS; Prpf3, pre-mRNA processing factor 3; RIP, RNA IP; RT–PCR, reverse transcription–PCR; RTT, Rett syndrome; Sdccag1, serologically defined colon cancer antigen 1; TRD, transcription repression domain.

[1] To whom correspondence should be addressed (email pjones@bbri.org).

methods utilized and non-neuronal choices for initial cellular protein sources. In fact, contradicting these numerous studies, it has been proposed that endogenous MeCP2 does not form any stable protein–protein interactions *in vivo* [19]. Compounding the issue, recent work has expanded MePC2's proposed gene regulatory role beyond mere transcriptional repression; MeCP2 is implicated in transcriptional activation, genome-wide transcriptional silencing, mediating chromatin and nuclear architecture, and regulating pre-mRNA splicing as well [20–23]. Thus the *in vivo* protein–protein interaction profile of endogenous MeCP2, particularly in the brain, is still an open question and increasingly more important to understand as new functions for MeCP2 are emerging.

Genetic studies in mice suggest that expression of functional MeCP2 in neurons is essential for normal synapse formation and neuronal function during postnatal development and re-expression of MeCP2 in differentiated neurons alone rescues an RTT mouse model [24–29]. However, this idea is being challenged by a recent study that indicates the lack of MeCP2 specifically in glial cells contributes to RTT phenotypic neurons by an unknown secreted glial factor [30]. This discrepancy illustrates the need for more unbiased approaches in determining the molecular roles of MeCP2 in both normal and RTT brain; thus, intact mammalian brain tissue would be the ideal source to study endogenous MeCP2 protein function. In the present study, we use the power of biochemistry to characterize MeCP2 in the mammalian brain and show that native MeCP2 protein purified from adult rat brain exists in multiple biochemically distinct pools/complexes, consistent with MeCP2 working as a multi-functional protein. We further characterize one brain-derived MeCP2 complex that contains Prpf3 (pre-mRNA processing factor 3), a known spliceosome-associated protein [31], as well as the Sdccag1 (serologically defined colon cancer antigen 1) [32], a mediator of nuclear export [33]. MeCP2 shows specific, direct interactions with Prpf3 and Sdccag1, and these interactions are disrupted by certain RTT mutations. In addition, we show that MeCP2 and Prpf3 co-associate *in vivo* with mRNAs from genes activated by MeCP2, further supporting the previously identified regulatory role of MeCP2 in mRNA biogenesis [23] and providing another potential mechanism disrupted during RTT pathogenesis.

MATERIALS AND METHODS

MeCP2 protein purification

Rat brain nuclei were isolated generally as described [34]. Adult rat brains ($n = 200$ per extract preparation; Pel-Freez Biologicals) were thawed on ice, homogenized and nuclei were collected. Nuclei were suspended in buffer A [20 mM Hepes (pH 7.5), 1.5 mM $MgCl_2$, 1 mM EGTA, 10 % glycerol, 0.5 mM DTT (dithiothreitol), 1 μg/ml leupeptin, 1 μg/ml pepstatin and 1 μg/ml aprotinin] supplemented with 350 mM NaCl (A-350) and extracted for 30 min at 4°C. Insoluble material was removed by centrifugation at 200000 ***g*** for 20 min at 4°C. The supernatant was diluted with buffer A to <200 mM NaCl and used as a soluble protein source for chromatography.

Chromatography was preformed using an AKTA-FPLC apparatus (GE Healthcare) at 4°C in buffer A with indicated concentrations of NaCl. Soluble protein (130 mg per purification) was fractionated over a MonoQ10/10 column with bound protein eluted by a 20 CV (column volume) linear salt gradient from 100 to 1000 mM NaCl, collecting 0.5 CV fractions. The MeCP2-containing fractions peaking at 230 mM NaCl (QB1/2) were pooled, diluted with buffer A and fractionated over MonoS5/5 with bound protein eluted by a 20 CV linear salt gradient from 250 to 1000 mM NaCl, collecting 0.5 CV fractions. The MeCP2 containing fractions peaking at 550 mM NaCl (QB2) were combined and loaded on to a 1 ml Heparin FastFlow column and eluted with a 10 CV linear gradient from 450 to 1000 mM, collecting 0.5 CV fractions. Pooled heparin column fractions containing MeCP2 were applied to a 110 ml Superose6 column and fractionated in buffer A-150 with 0.1 % Triton X-100. Subsequently, 0.5 ml of each fraction was trichloroacetic acid-precipitated, subjected to SDS/PAGE, and used for Western blotting or silver staining. Silver-stained polypeptide bands precisely co-fractionating with MeCP2 (by Western blotting) were excised and analysed by MS.

For the nuclease treatment experiments, MonoQ-eluted MeCP2 was dialysed against buffer A-100 containing 1 mM $CaCl_2$, 10 mM $MgCl_2$ and without EGTA then either treated with or without 500 units of benzonase nuclease (Sigma) for 30 min at 37°C, and re-tested for ability to bind the MonoQ resin.

Antibodies and Western blot analysis

Protein samples were separated by SDS/PAGE and transferred to ECL nitrocellulose membrane (GE Healthcare) for Western blotting by standard methods. For each experiment, the Western blotting images presented are from the same exposure on the same piece of film, linearly adjusted for brightness in Adobe Photoshop. The anti-MeCP2 3998 antibody is a rabbit polyclonal antibody derived from bacterially expressed recombinant protein encoding the full-length human MeCP2e2 isoform. The anti-(MeCP2 7–18) antibody is a rabbit polyclonal derived from bacterially expressed recombinant protein encoding amino acid residues 310–388 of the human MeCP2e2 isoform. Antibodies were used at the following concentrations: anti-(MeCP2 7–18), 1:2000; anti-MeCP2 (Upstate 07–013) 1:1000; anti-Prpf3 (MBL D171–3) 1:2000; and anti-HA (haemagglutinin) high affinity (clone 3F10) at 1:1000.

Mass spectrometry

MS was carried out at the Protein Sciences Facility at the University of Illinois. FPLC-purified fractions were separated by SDS/PAGE, visualized by MS-compatible silver staining. Polypeptide bands were excised, destained (50 % acetonitrile and 25 mM ammonium bicarbonate) and digested in 25 μl of Sequencing Grade Trypsin (12.5 ng/μl in 25 mM ammonium bicarbonate, G-Biosciences St Louis, MO, U.S.A.) using a CEM Discover Microwave Digestor for 15 min at 55°C (60W). Digested peptides were extracted using 50 % acetonitrile with 5 % formic acid, dried in a Savant SpeedVac apparatus and suspended in 13 μl of 5 % acetonitrile containing 0.1 % formic acid with 10 μl of sample

used for MS analysis. The mass spectrometer used was a Waters quadrupole time-of-flight (Q-ToF) mass spectrometer connected to a Waters nano-Acquity UPLC. The column used was Waters Atlantis C_{18} (0.075 mm × 150 mm) with a flow rate of 250 nl/min. Peptides were eluted using a linear gradient of water/acetonitrile containing 0.1 % formic acid (0–60 % B) in 60 min. The mass spectrometer was set for result-dependent acquisition; MS/MS (tandem MS) was performed on the most abundant four peaks at any given time. Data analysis was performed using Waters Protein Lynx Global Server 2.2.5, Mascot (Matrix Sciences) and BLAST against NCBI NR database.

Generation of plasmids

RNA was purified from rat brain tissue or HeLa cells using TRIzol® Reagent (Invitrogen) as per the manufacturer's instructions. All cDNAs were generated using SuperScript III one-step RT (reverse transcription)–PCR with Platinum Taq (Invitrogen). All PCRs were performed with Phusion polymerase (New England Biolabs) and cloned into pGEM-T easy (Promega) for sequencing before subcloning into pGEX5-X1 (GE Life sciences), pCDNA 3.1 (Invitrogen) or the pCDNA 3.1 HA vector [35]. All primers are listed in Supplementary Table S1 (at http://www.bioscirep.org/bsr/031/bsr0310333add.htm). All human MeCP2 constructs were generated from the human *MECP2E2* cDNA (NM_004992). To generate constructs for *in vitro* synthesized proteins, cDNAs were PCR-amplified using primers listed in Supplementary Table S1 and subcloned into the specified restriction sites of pCDNA 3.1. Rat cDNAs were subcloned between NotI and XhoI; the human Prpf3 cDNA clone was subcloned between EcoRI and XhoI; the human full-length MeCP2 was amplified from full-length cDNA and subcloned between NotI and XhoI. Constructs for bacterially generated GST (glutathione transferase) fusion proteins were PCR-amplified from full-length cDNAs, subcloned into the specified restriction sites of pGEX5-X1 using primers listed in Supplementary Table S1. Rat GST–Prpf3 was subcloned between BamHI and XhoI. The rat and human GST–MeCP2 full-length, GST–MeCP2 deletion and human GST–MeCP2 RTT cDNAs were subcloned between EcoRI and XhoI. For the pCDNA3PHA-MECP2 vector, full-length human MeCP2 was subcloned between NotI and XhoI restriction sites of the pCDNA3.1 HA vector and subsequent digestion with NdeI and XhoI for cloning of the HA–MeCP2 fragment into the pCDNA3.1P puromycin vector.

Cell culture

HT-22 cells were transfected with pCDNA 3.1P HA-MeCP2 using Fugene HD transfection reagent (Roche). Stable integrants were selected as pools in puromycin (1 μg/ml), and maintained in DMEM (Dulbecco's modified Eagle's medium; Biowhittaker) supplemented with 10 % fetal bovine serum, glutamine, antibiotics and puromycin.

GST pull-down assay

Assays were preformed essentially as previously described [35], using recombinant GST fusion proteins and *in vitro* transcribed/translated proteins radiolabelled with [^{35}S]methionine using the T7 TnT Quick Coupled Transcription/Translation System (Promega) with or without 250 units of Benzonase nuclease.

Co-IP (co-immunoprecipitation)

Co-IPs from fractionated brain extracts were carried out as follows: MonoQ-fractionated rat brain nuclear extracts (QB2) were diluted to 100 mM NaCl with buffer A (0). Protein A Dynabeads (Invitrogen) were blocked with BSA and added to the extracts with 10 μl of either anti-MeCP2 3998 or normal rabbit serum IgG for 2 h at 4°C with rotation. Co-immunoprecipitates were washed three times with buffer A225, eluted by boiling in Laemmli buffer, separated by SDS/PAGE and subjected to Western-blot analysis. Co-IPs from cell culture were carried out as previously described [23] with modifications. Confluent 10-cm plates of HT-22 cells stably expressing HA–MeCP2 were lysed in 1 ml of IPH buffer [50 mM Tris/HCl (pH 8.0), 150 mM NaCl, 5 mM EGTA, 0.5 % Igepal and 1 mM PMSF] and debris removed by centrifugation. Lysates were pre-cleared with Protein A agarose, then incubated for 4 h with anti-HA (Sigma, E6779) or irrelevant IgG with Protein A agarose beads (Santa Cruz Biotechnologies) at 4°C with rotation. Nuclease treatment was preformed by suspension of protein-bound beads with 125 units of benzonase in the manufacturer's recommended buffer for 10 min at 37°C. IPs were washed three times with IPH buffer, eluted with Laemmli buffer, separated by SDS/PAGE and subjected to Western-blot analysis.

RIP (RNA IP) and Re-RIP

Experiments were performed as previously described with slight modifications [36]. HT-22 cells (10^8) stably expressing HA–MeCP2 were collected, washed and suspended in 4 ml of PBS. Cross-linking buffer (50 mM Hepes, 100 mM NaCl, 1 mM EDTA, 0.5 mM EGTA and 11 % formaldehyde) was added (400 μl), incubated at room temperature (23°C) for 30 min with rocking and quenched for 5 min at room temperature. Cell pellets were washed with PBS and lysed in 1 ml of FA buffer [50 mM Hepes/KOH (pH 7.5), 140 mM NaCl, 1 mM EDTA, 1 % Triton X-100, 0.1 % sodium deoxycholate and protease inhibitors] by sonication. The lysed cells were treated with 200 units of DNase I (Promega) in 25 mM $MgCl_2$, 5 mM $CaCl_2$ and 6 μl of RNasin (Promega) for 30 min at 37 °C, cleared by centrifugation at 4°C, diluted 1:10 with ChIP (chromatin immunoprecipitation) dilution buffer [50 mM Hepes (pH 7.5), 140 mM NaCl, 1 mM EDTA, 10 % glycerol and 0.5 % Nonidet P40] and incubated with either anti-HA antibody or non-specific IgG with 4 μl of RNasin, for 12 h, rotating at 4°C. Protein A or G Dynabeads were added for 1 h rotating at 4°C and washed three times for 10 min each with wash buffer [50 mM Tris/HCl (pH 7.4), 500 mM NaCl, 1 % Triton X-100 and 0.1 % SDS]. For Re-RIP experiments, beads were washed and bound immune-RNA complexes were released in 20 mM DTT for 30 min at 37°C and resuspended in 1 vol. of ChIP dilution buffer for Re-RIP with antibody for Prpf3 and washed as described above. Beads were brought up in 200 μl of elution buffer [50 mM Tris/HCl (pH 7.4), 200 mM

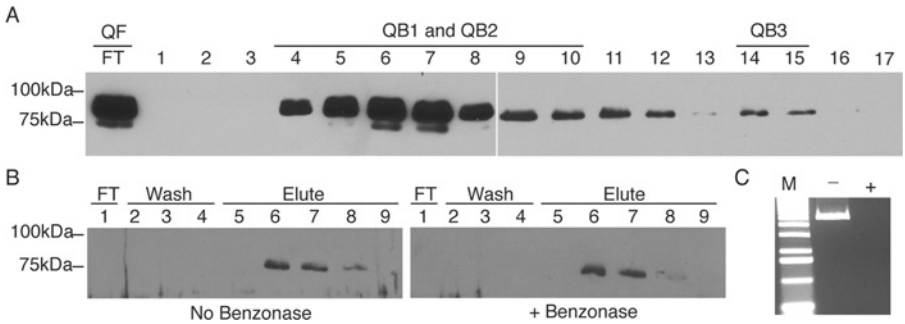

Figure 1 Brain-derived nuclear MeCP2 exists in multiple biochemically distinct pools

(A) Chromatographic separation of crude rat brain nuclear extract by strong anion exchange (MonoQ resin) results in three distinct pools of MeCP2 as indicated by Western-blot analysis using the MeCP2 7–18 antibody (Figure S1). The majority of MeCP2 does not bind the column (QF), whereas the bound MeCP2 elutes in two peaks, at 230 mM NaCl (QB1/2) and 450 mM NaCl (QB3). (B) MonoQ-resin-bound fractions of MeCP2 were treated with (+) or without (No) benzonase nuclease and tested for ability to re-bind the Mono Q. Western-blot analysis for MeCP2 of MonoQ flow through, wash, and 1000 mM NaCl step elution shows that benzonase treatment does not affect binding of MeCP2 to the Mono Q column. (C) Plasmid spiked MonoQ fractions treated with benzonase (+) or untreated (−) in parallel served as controls for benzonase treatment.

NaCl and 20 μg of proteinase K] for 1 h at 42°C, and cross-links reversed at 65°C. Samples were extracted with acid-equilibrated (pH 4.8) phenol/chloroform (5:1, v/v) and ethanol-precipitated. Precipitated material was suspended in 50 μl of DEPC (diethyl pyrocarbonate)-treated water and used for RT–PCR analysis with SuperScript III One-Step RT–PCR with Platinum Taq (Invitrogen) for mouse Cdk10 (cyclin-dependent kinase 10) and Frg1. Reaction mixtures were analysed by electrophoresis on a 2% agarose gel.

RESULTS

MeCP2 exists in at least four distinct protein pools in rat brain nuclei

A large-scale biochemical purification of endogenous MeCP2 protein from rat brain nuclear extract was performed to characterize the native MeCP2 in the mammalian brain. Whole rat brains were homogenized under non-denaturing conditions, the intact nuclei were purified by centrifugation through a sucrose cushion, and nuclear proteins were extracted under mild ionic conditions. Proteins were initially fractionated by strong anion exchange (MonoQ) column chromatography with the MeCP2 protein being tracked by Western blotting with multiple MeCP2-specific antibodies (Figure 1A and Supplementary Figure S1 at http://www.bioscirep.org/bsr/031/bsr0310333add.htm; and results not shown), all providing virtually identical profiles. The majority of soluble MeCP2 protein (~90%) did not associate with the MonoQ resin agreeing with a previous report [19]; however, a significant fraction (~10%) of this brain-derived MeCP2 consistently bound to MonoQ resin and was eluted in two distinct peaks along the linear salt gradient (Figure 1A), indicating multiple biochemically distinct pools of MeCP2.

The MonoQ bound (QB) MeCP2 elution profile showed an initial broad peak (QB1/2) concentrated at 230 mM NaCl and tailing to 370 mM, suggesting multiple MeCP2 complexes, with a minor yet distinct peak (QB3) centred at 450 mM NaCl (Figure 1A). Since MeCP2 is a DNA-binding protein and also known to interact with RNA, the potential of nucleic acids mediating the anionic association of MeCP2 with the cationic resin was addressed. The QB fractions were treated with benzonase nuclease to remove both DNA and RNA and then MonoQ chromatography was repeated. We found that all of the nuclease-treated QB MeCP2 still bound the MonoQ resin and was released by step elution, indicating the interaction was both RNA and DNA independent (Figures 1B and 1C). Finally, the presence of MeCP2 in the MonoQ flow through (QF) and each elution peak (QB1/2 and QB3) was subsequently confirmed by MS (Supplementary Figure S2 at http://www.bioscirep.org/bsr/031/bsr0310333add.htm).

The early eluting MonoQ-bound pool of MeCP2 (QB1/2) was characterized further for complexity and content (Figure 1A). The QB1/2 peak fractions were pooled and fractionated over the MonoS strong cation exchange resin, resolving into two peaks of MeCP2 protein (Figure 2D, top panel), the first being eluted at 400 mM NaCl (QB1) and the second being eluted at 550 mM NaCl (QB2). These results indicate at least three biochemically distinct pools of MeCP2 exist in the initial QB fraction and four MeCP2 pools exist overall in rat brain nuclear extract (QF and QB1, QB2 and QB3).

Brain-derived MeCP2 exists in a complex with the splicing factor Prpf3

To identify potential MeCP2-interacting proteins, the more abundant MonoS-bound pool of MeCP2 (QB2) was purified further by fractionation using heparin affinity chromatography and gel filtration through Superose6 (Figure 2A). Western blotting and silver-stain analysis of the final fractionation showed MeCP2 peaking with an apparent molecular mass of 600–700 kDa and precisely co-purifying with six additional polypeptides (Figures 2B and 3). Since monomeric MeCP2 has previously been shown to exhibit an unusual Superose6 gel filtration profile migrating equivalent with an apparent mass of approx. 450 kDa [19], the apparent mass for QB2 MeCP2 is consistent with it

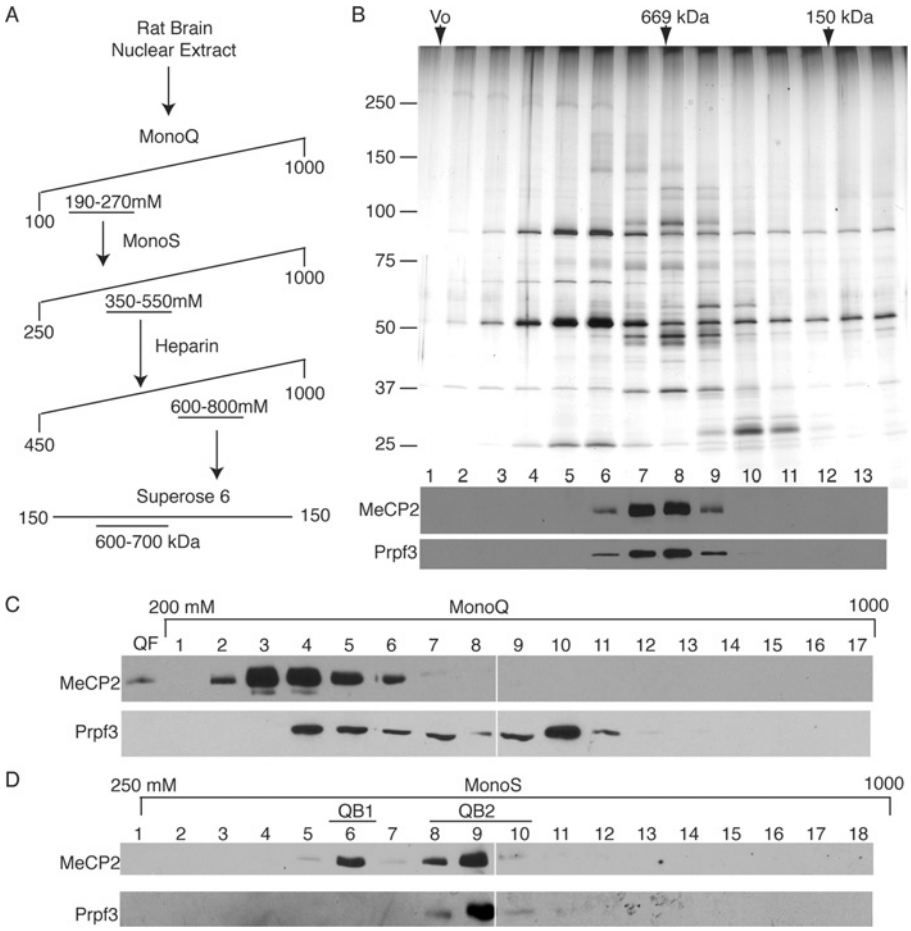

Figure 2 The QB2 pool of MeCP2 co-purifies with six candidate proteins including Prpf3
(A) MeCP2 peak fractions were purified using a four-step process including the MonoQ strong anion exchange resin, MonoS strong cation exchange resin, Heparin affinity resin and by Superose6 gel filtration. (B) (Upper panel) Silver-stain analysis of the Superose6 fractionation of the QB2 MeCP2 pool. (Lower panel) Western-blot analysis of Superose6 fractions shows MeCP2 protein peaks in fractions 7 and 8, precisely co-fractionating with Prpf3 protein. (C) The MonoQ fractionation of brain-derived nuclear extract reveals an overlap of Prpf3 and MeCP2 yet pools of each protein do not co-fractionate and remain independent of the other. (D) Peak fractions of the QB1/2 fractionated over the MonoS resin show two distinct pools of MeCP2 peaking at 400 mM NaCl (QB1) and 550 mM NaCl (QB2) by Western-blot analysis. Corresponding MonoS fractions probed for Prpf3 protein shows precise co-fractionation with QB2 Mecp2.

being associated with additional proteins. Therefore all six MeCP2 co-purifying polypeptides were identified by MS with significant coverage (Figure 3 and Supplementary Figure S3 at http://www.bioscirep.org/bsr/031/bsr0310333add.htm) as Prpf3, Sdccag1, ATP-binding cassette 50 and three components of a translation initiation complex (Eif2 subunits 1, 2 and 3). Since a commercial antibody was available against Prpf3, Western-blot analysis of the size exclusion chromatography fractions was carried out and showed that MeCP2 and Prpf3 precisely co-fractionate (Figure 2B, bottom) confirming the silver-stain analysis (Figure 2B, top).

With Prpf3 identified as a putative MeCP2-interacting protein, the MeCP2 fractionation scheme (Figure 2A) was analysed for Prpf3 by Western blotting to determine whether Prpf3 was present in all MeCP2 pools or specific to QB2 and similarly to determine whether all Prpf3 in brain extracts associated with MeCP2. Not surprisingly, only a fraction of Prpf3 in brain extracts co-fractionated with MeCP2 when assaying the MonoQ separation profile (Figure 2C); however, all of the detectable Prpf3 overlapping with MeCP2 specifically co-fractionated with the QB2 pool of MeCP2 from the MonoS fractionation and not with the QB1 MeCP2 pool (Figure 2D). Thus Prpf3 distinguished QB2 from other MeCP2 protein pools. Because Prpf3 is a known component of the spliceosome [31] and MeCP2 has been shown to interact with another spliceosome-associated protein, YB-1 [23], the QB2 fractionation was screened for YB-1. However, YB-1 was not found by Western blotting and YB-1 was absent from the MS analysis indicating YB-1 did not co-purify with QB2 MeCP2 under these conditions (Figure 3, and results not shown).

To confirm that native MeCP2 and Prpf3 are in a complex *in vivo*, co-IP experiments were performed (Figure 4). In brain extracts, as determined by the biochemical fractionations described

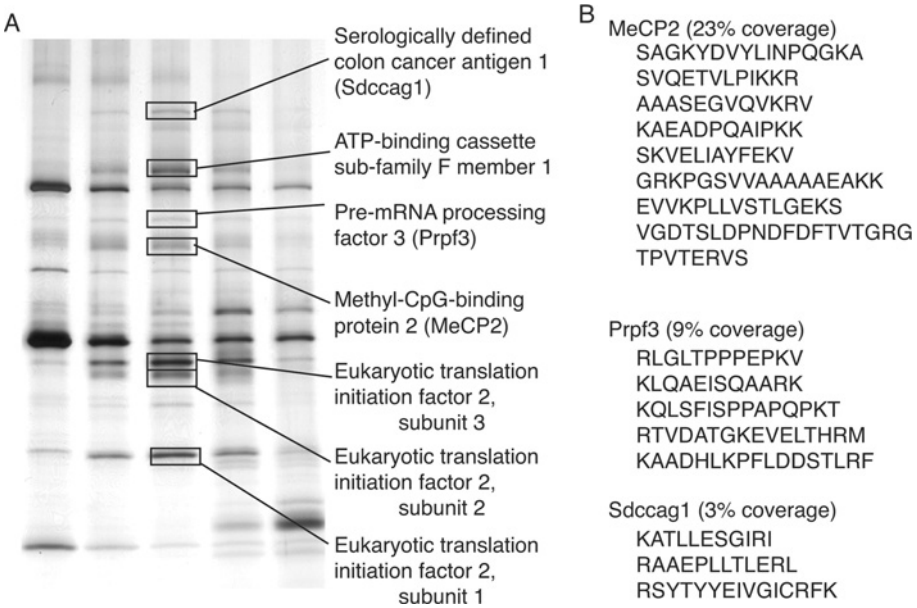

Figure 3 **Identification of candidate MeCP2 complex proteins**
(A) Polypeptides from silver-stained Superose6 fractions were excised and identified by LC (liquid chromatography)-MS/MS. MeCP2 and two other nuclear proteins, Sdccag1 and Prpf3, were identified as well as components of a translation initiation complex. (B) MS peptides identifying MeCP2, Prpf3 and Sdccag1.

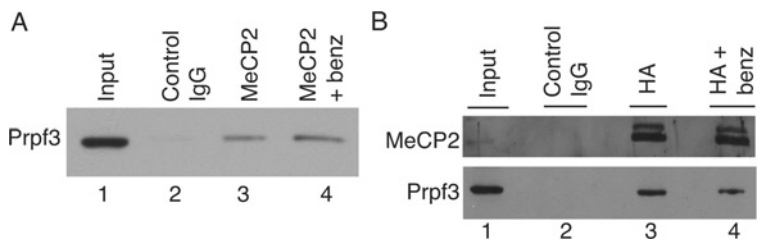

Figure 4 **Co-IPs confirmed MeCP2 associates with Prpf3 *in vivo***
(A) Western blotting of a co-IP experiment from fractionated brain extract showing a peak MeCP2 fraction (lane 1, 5% input), control IgG IP (lane 2), anti-MeCP2 IP (lane 3) and anti-MeCP2 IP treated with benzonase (benz) (lane 4) demonstrates that Prpf3 interacts with MeCP2 in the brain independent of nucleic acids. (B) Western blotting of a co-IP experiment from HA–MeCP2 transfected HT-22 cells showing whole-cell extract (lane 1, 5% input), IgG IP (lane 2), anti-HA IP (lane 3) and anti-HA IP treated with benzonase (lane 4) demonstrates that Prpf3 interacts with MeCP2 cell culture independent of nucleic acids.

above, the vast majority of MeCP2 is not associated with Prpf3 and likewise the majority of Prpf3 in brain is not associated with MeCP2 making it difficult to visualize any interaction by co-IP directly from crude nuclear extracts. Thus two approaches were used: co-IPs from fractionated brain nuclear extract (Figure 4A) and co-IPs from crude extracts using tissue culture cells overexpressing an epitope-tagged version of MeCP2 (Figure 4B). Rat brain nuclear extract was prepared and fractionated over MonoQ as described above. The QB1/2 MeCP2 fractions were diluted to 100 mM NaCl in buffer A (0) and used for co-IP experiments assayed by Western blotting. Using the anti-MeCP2 3998 antibody to IP, Prpf3 was specifically co-immunoprecipitated from these fractions and the interaction between MeCP2 and Prpf3 was not dependent on nucleic acids (Figure 4A, lanes 3 and 4). Alternatively, to show co-IP interaction between MeCP2 and Prpf3 from crude cell extracts, the murine hippocampal HT-22 cell line was used to generate a pool of cells stably expressing HA epitope-tagged human MeCP2. Immunofluorescence showed that HA–MeCP2 in these cell lines predominantly concentrated to DAPI (4′,6-diamidino-2-phenylindole)-rich heterochromatic foci as expected for endogenous MeCP2 (supplemetnary Figure S4 at http://www.bioscirep.org/bsr/031/bsr0310333add.htm). Anti-HA antibodies were then used to specifically co-IP HA–MeCP2 and MeCP2-associated proteins from these cell lines. Western blotting showed that HA–MeCP2 specifically co-immunoprecipitated a fraction of the endogenous mouse Prpf3 (Figure 4B, lane 3), indicating that Prpf3 and MeCP2 exist in a stable complex within these neuronal cells, and their interaction

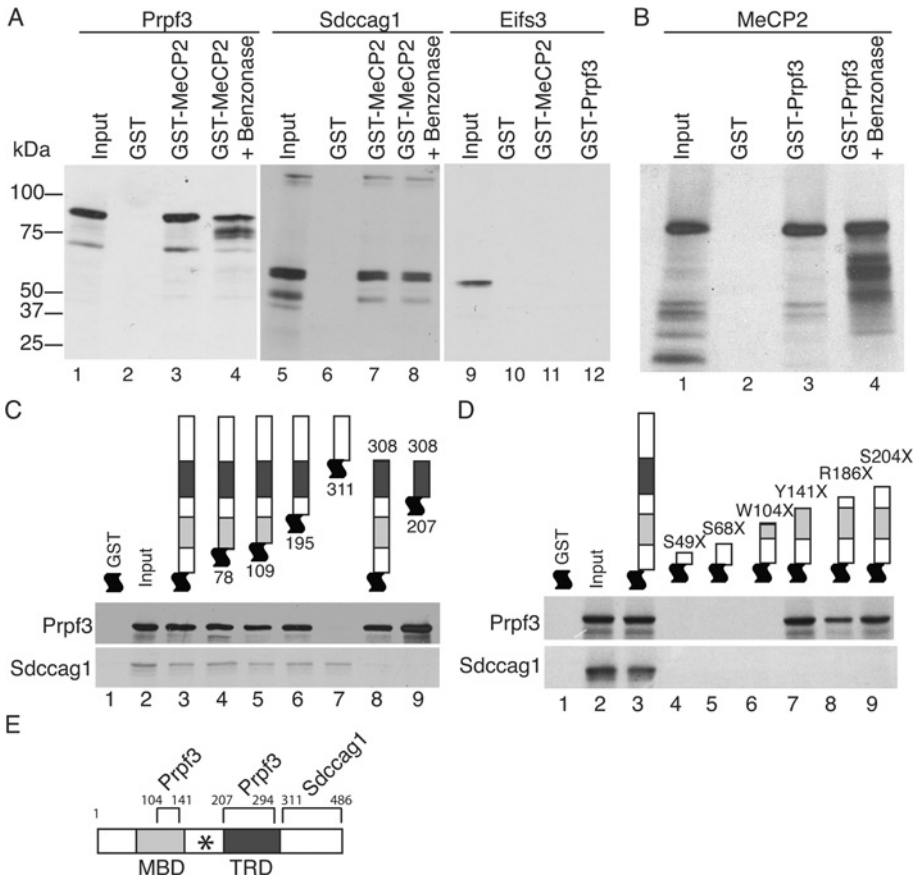

Figure 5 MeCP2 directly interacts with Prpf3 and Sdccag1

For all experiments, the GST-tagged protein was bacterially generated and purified and the visualized [^{35}S]methionine-labelled interacting proteins were generated by *in vitro* transcription and translation. Coomassie Brilliant Blue staining of the gels showing input GST fusion proteins are shown in Supplementary Figure S4 at http://www.bioscirep.org/bsr/031/bsr0310333add.htm. (A) Prpf3 (left) and Sdccag1 (middle) interact directly with GST-tagged MeCP2 but not GST alone. Eif2s3 (right) does not interact with either GST–MeCP2 or GST–Prpf3. Benzonase treatment indicates these interactions are independent of nucleic acids. (B) Reciprocally, MeCP2 interacts with GST-tagged Prpf3 independent of nucleic acids. (C) GST–MeCP2 deletion constructs mapped the region of MeCP2 required for the direct interactions with Prpf3 or Sdccag1 *in vitro*. (D) GST-tagged MeCP2 containing the indicated RTT non-sense mutations disrupt Prpf3 binding if truncations are before amino acid 104, but identify a second Prpf3-binding site on MeCP2 in the MBD between amino acids 104 and 141. All RTT truncations tested abolished Sdccag1 binding to MeCP2. (E) Map of MeCP2e2 protein showing the Prpf3 and Sdccag1 interaction domains with boundary amino acid numbers. The MBD, TRD and RNA-binding domain (*) [37] are indicated.

was not dependent on nucleic acids (Figure 4B, lane 4). We conclude that MeCP2 and Prpf3 associate *in vivo*.

MeCP2 interacts directly with Prpf3 and Sdccag1, independent of nucleic acids

To investigate which of the co-purifying candidate proteins directly interacted with MeCP2, the cDNAs for each identified protein was cloned and the recombinant proteins were tested for the ability to interact with MeCP2 *in vitro* (Figure 5 and Supplementary Figure S4). GST pull-down assays using a GST–MeCP2 fusion protein showed that rat Prpf3 specifically interacted with full-length rat MeCP2, but not GST alone (Figure 5A, left panel), and reciprocally rat GST–Prpf3 interacted with rat MeCP2 (Figure 5B). Furthermore, treatment of the GST–MeCP2/Prpf3 reaction with benzonase nuclease showed the interaction was not dependent on nucleic acids (Figure 5A and 5B). Similarly, rat Sdccag1 specifically interacted with rat GST–MeCP2 in a nucleic acid-independent manner (Figure 5A, middle panel). Interestingly, neither rat GST–MeCP2 nor rat GST–Prpf3 interacted with any of the other four identified polypeptides supporting the specificity of the observed interactions of MeCP2, Prpf3 and Sdccag1 (Figure 5A, right panel, and results not shown).

Mapping the Prpf3 and Sdccag1 interaction domains of MeCP2

The regions of MeCP2 that directly interact with Prpf3 and Sdccag1 were mapped by GST pull-down analysis. A series of bacterially generated human GST–MeCP2 deletion mutants were

tested for their ability to interact with *in vitro* synthesized human Prpf3 (Figures 5C and 5D). Prpf3 retained the ability to interact with MeCP2 N-terminal deletions up to and including amino acid residue 195 as well as a C-terminal deletion lacking amino acid residues 309–486. However, Prpf3 did not interact with an MeCP2 deletion lacking amino acid residues 1–308, indicating that the TRD (transcription repression domain) region is required for interaction (Figure 5C, upper panel). Therefore a fragment of MeCP2 that contains only amino acid residues 207–308, corresponding to the TRD domain, was tested and found to interact with Prpf3 with similar apparent affinity as full-length MeCP2. Similarly, Sdccag1 was synthesized *in vitro* and subjected to the same series of GST–MeCP2 deletions as Prpf3 (Figure 5C, lower panel). Sdccag1 was capable of interacting with all of the N-terminal MeCP2 deletion proteins tested, but failed to interact with a MeCP2 deletion lacking the region C-terminal to the TRD. Thus the interaction domain with Sdccag1 resides between amino acid residues 309 and 486, adjacent with the Prpf3 interaction domain (Figure 5E).

Considering most known RTT mutations reside in *MECP2* and many are nonsense mutations resulting in a truncated MeCP2, it is likely that some of these mutations would also disrupt the interactions of Prpf3 and/or Sdccag1 with MeCP2. A series of bacterially generated human GST–MeCP2 RTT nonsense mutants were produced and tested for their ability to interact with *in vitro* synthesized human Prpf3 and rat Sdccag1 (Figure 5D). The series of RTT mutations truncate MeCP2 ranging from amino acids 49 to 204. All of these RTT nonsense mutants lack the C-terminal region of MeCP2 and therefore disrupted its interaction with Sdccag1 as expected (Figure 5D, bottom panel). The Prpf3 interaction was disrupted by RTT truncations at amino acids S49X, S68X and W104X as well. However, the Prpf3 interaction with MeCP2 was maintained with the RTT truncations Y141X, R168X and S204X. This indicates there are two MeCP2 regions capable of interacting with Prpf3 flanking the inter-domain region between the MBD and TRD of MeCP2. Interestingly, this same inter-domain region of MeCP2 has been previously characterized as the RG domain and is required for MeCP2's RNA-binding activity [37]. We conclude that MeCP2 contains two domains sufficient for interaction with Prpf3, one in the MBD between amino acids 104 and 141, and the second in the TRD between amino acids 207 and 294 and one domain for MeCP2's interaction with Sdccag1, residing between amino acids 311 and 486 (Figure 5E). Therefore any RTT mutation truncating MeCP2 at or before amino acid residue 104 will abolish the Prpf3 and Sdccag1 interaction, whereas any RTT truncation at or before amino acid residue 297 would disrupt the Sdccag1 interaction with MeCP2, all of which could affect MeCP2's role in RNA biogenesis.

MeCP2 interacts with mRNA *in vivo*

Several lines of evidence suggest that MeCP2 is associated with mRNA biogenesis; MeCP2 binds RNA *in vitro* [37], is part of an RNP complex with YB-1 in cell culture [23], MeCP2 knockout mice show mis-spliced transcripts in the brain [23], it has been identified as a transcriptional activator at the majority of gene promoters it has been shown to regulate [21], and in the present study MeCP2 was shown to interact with the splicing factor Prpf3. To determine whether MeCP2 interacts with the RNA transcripts expressed from the genes it regulates *in vivo*, RIPs were performed. Using anti-HA antibodies on HT-22 (HA–MeCP2) cell lysates, mRNAs for the MeCP2-regulated genes *Cdk10* and *Frg1* were capable of being specifically RNA immunoprecipitated (Figure 6A). Assaying the IPs by RT–PCRs using oligonucleotide primers designed to amplify across exon junctions of *Cdk10* and *Frg1* show that MeCP2 is associated with the spliced form of the genes, whereas MeCP2 is not associated with the *Casc3* gene transcript (Figure 6A), a gene not regulated by MeCP2 [21], supporting the specificity of the MeCP2–mRNA interaction. The RIPs were RNase sensitive confirming that RNA, and not DNA, was specifically immunoprecipitated. Interestingly, RT–PCR for RIPs using primers for *Cdk10* additionally show what appears to be pre-mRNA by size and RNase sensitivity (Figure 6A, top). Although the *Cdk10* pre-mRNA product was not observed in 100 % of the RT–PCR analyses for *Cdk10*, it was observed repeatedly and suggests that MeCP2 associates with the *Cdk10* RNA at a step before the completion of splicing and remains bound after RNA processing is completed.

To investigate whether Prpf3 was part of the HA–MeCP2–mRNA complex, an RIP and Re-RIP approach was implemented. Anti-HA antibodies were used to RNA immunoprecipitate HA–MeCP2–mRNA complexes from HT-22 (HA–MeCP2) cell lysates, the bound complexes were eluted from the HA antibodies intact using DTT to disrupt the IgG structure and then anti-Prpf3 antibodies were used to Re-RIP. Therefore any RNAs present in the Re-RIP must have been associated with both MeCP2 and Prpf3. RT–PCR analysis showed that RIP for HA–MeCP2 and subsequent Re-RIP for Prpf3 protein immunoprecipitated mRNA for *Cdk10*, indicating that both proteins are in fact associated with this target mRNA (Figure 6B), further supporting their being in a complex *in vivo*.

DISCUSSION

MeCP2 has been characterized as a multifunctional protein using a variety of techniques and from numerous cellular contexts; however, only the biochemical characteristics of the endogenous MeCP2 protein in the mammalian brain are relevant to RTT. MeCP2 mutations identified from RTT patients are generally point mutations resulting in a single missense or non-sense amino acid change, and have been identified throughout all protein domains of *MECP2* (http://www.rettsyndrome.org/), suggesting that all domains are critical for MeCP2 function [38]. Although all these mutations produce clinical RTT pathology, certain mutations are more strongly associated with particular symptoms and disease severity suggesting that all RTT mutations in *MECP2* are not equal, with some potentially being more disruptive towards MeCP2's many functions [39]. The underlying mechanisms of how these myriad mutations lead to RTT pathophysiology

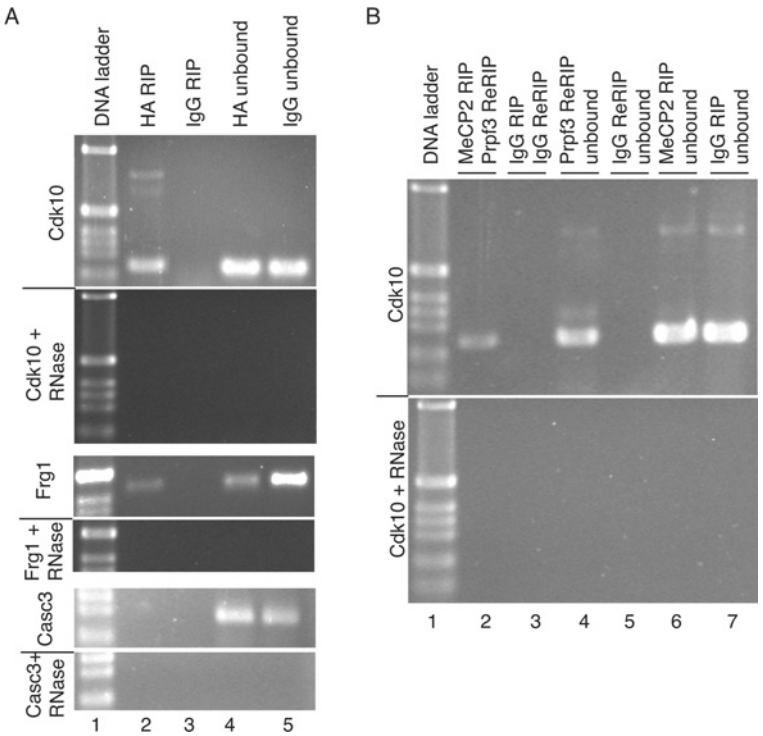

Figure 6 The MeCP2–Prpf3 complex interacts with mRNA *in vivo*
(A) RT–PCR analysis of a RIP from HA–MeCP2 stably transfected HT-22 cells indicates an association of HA–MeCP2 with Cdk10 mRNA (top, lane 2) and FRG1 mRNA (middle, lane 2), but not Casc3 mRNA (bottom, lane 2). Control RIPs using normal rabbit serum (IgG) (lane 3) show no RT–PCR product. RT–PCRs using unbound RNA from RIPs indicate target mRNAs were present in all RIP samples (lanes 4 and 5) and all RT–PCRs were RNase sensitive (+RNase) confirming RNA and not DNA was being assayed. (B) An anti-HA RIP followed by anti-Prpf3 Re-RIP experiment from HA–MeCP2 HT-22 cells was assayed for Cdk10 mRNA by RT–PCR (lane 2). Control RIP and Re-RIP experiments using normal rabbit serum (IgG) showed no product by RT–PCR (lane 3). Unbound mRNA was assayed by RT–PCR for the RIP (lanes 6 and 7) and Re-RIPs (lanes 4 and 5) to confirm the presence of the Cdk10 mRNA in the reaction mixtures. All RT–PCRs were sensitive to RNase treatment (lower panel) confirming the amplifications were from RNA and not DNA templates.

remain unclear due to a lack of understanding towards the complete scope of MeCP2's normal function in the brain. In the present study, we identified four distinct brain-derived MeCP2 protein pools, agreeing with the functional results proposing multiple roles for MeCP2 [38]. Characterizing one complex as containing MeCP2, Pprf3, Sdccag1 and mRNA strongly complements previously published results that MeCP2 is an RNA-binding protein involved in mRNA splicing [23].

MeCP2's association with Prpf3, a major component of the spliceosome, supports MeCP2 as having a role in modulating mRNA splicing [23]; however, it is not clear what exactly that role might be. MeCP2 is present at the promoter of many actively transcribed genes [20], and activates a majority of genes it regulates in the mouse hippocampus [21]. Interestingly, a recent study suggests that differential gene body methylation may play a role in RNA transcript splicing [40]. Genome-wide methylation profiling in multiple human cell types found that exons were more highly methylated than introns, and that there were sharp transitions of DNA methylation at exon–intron boundaries [40]. Experimentally, it is known that MeCP2 binds RNA *in vitro* with an affinity similar to that of methylated DNA, and that the two activities are mutually exclusive [37]. Thus MeCP2 at an active promoter or within the body of a transcribed gene would be well positioned spatially on its release to interact with the transcripts of the genes it activates and influence splice site selection. Therefore it is reasonable to propose that MeCP2-activated genes would also be targets for splicing regulation by an MeCP2 containing complex. Supporting this model, RNA transcripts from *Cdk10*, a gene positively regulated by MeCP2 binding at its promoter [21] and abnormally spliced in *Mecp2*^{308Y} mice [23], were associated with both MeCP2 and Prpf3 *in vivo* (Figure 6).

Based on what is known about MeCP2 and Prpf3 independently, it is possible that the direct interaction of MeCP2 with Prpf3 could function in splice site selection. Prpf3 is one of multiple associated proteins of the U4/U6.U5 tri-snRNP (tri-small nuclear ribonucleoprotein) complex that is recruited to the splice site to form and stabilize the functional spliceosome, and is essential for pre-mRNA splicing [31,41]. Importantly, MeCP2 can bind RNA directly [37] and has been implicated as a regulator of alternative splicing in the HeLa and Neuro2A cell lines through an RNA-dependent interaction with YB-1 [23], a protein known to participate in splicing of mRNAs [42]. Although we were unable

to detect YB-1 as a component of the MeCP2–Prpf3–Sdccag1 complex in brain, it is inefficient to inhibit the highly active and stable RNases that would abolish any YB-1–RNA–MeCP2 interaction during purification, hence we cannot rule out that YB-1 could be part of a larger RNA-dependent alternative splicing complex. Nevertheless, a direct interaction of MeCP2 and Prpf3 further supports a role for MeCP2 in mRNA splicing regulation. Notably, *Mecp2*$^{308/Y}$ mice, which produce a truncated form of MeCP2 and reproduce many of the classical features of RTT [43], have been shown to have multiple genes that are abnormally spliced in the brain [23]. This suggests the C-terminal portion of MeCP2, which we have identified as the putative Sdccag1 interaction domain, plays a critical role in regulating alternative splicing.

Sdccag1 was originally identified from colon cancer patients by a serological analysis of recombinant cDNA expression libraries (SEREX) [32] and later identified as a tumour suppressor by its ability to cause cell cycle arrest in a non-small-cell lung cancer cell line [44]. The significance of finding Sdccag1 as part of the MeCP2–Prpf3 complex can only be implied due to the limited information on its function in vertebrates and *Drosophila*. Bioinformatically the Sdccag1 protein contains a predicted RNA-binding domain homologous with a eukaryotic small nuclear RNP [45], suggesting the capacity to function in mRNA splicing. Functionally, the *Drosophila* Sdccag1 homologue Caliban has been shown to interact with and mediate the nuclear export of the Prospero homeodomain transcription factor (Prox in mammals) and this interaction and function is conserved in mammalian cells [33]. This raises the possibility that the MeCP2–Prpf3–Sdccag1 complex may not only be involved in splicing mRNA but also transporting mRNAs. Consistent with this model, MeCP2 has been shown to have both a nuclear and cytoplasmic localization in neuronal cell lines [46].

Considering the range of mutations throughout *MECP2* in RTT, it is not surprising that many RTT mutations are within, or predicted to affect both the Prpf3- and Sdccag1-binding domains, disrupting the MeCP2–Prpf3–Sdccag1 complex and presumably MeCP2-mediated splicing regulation and mRNA transport. With MeCP2 emerging as a multifunctional protein and its biological role in RTT unclear, identifying biochemically distinct pools of MeCP2 in the brain containing novel MeCP2-interacting proteins is a valuable tool towards an understanding MeCP2 function and its dysfunction in RTT. The present study adds to the mounting evidence indicating that one such critical function of MeCP2 in the brain involves RNA biogenesis.

AUTHOR CONTRIBUTION

Steven Long performed the biochemistry, IPs, co-IPs, RIPs, transfections and wrote the paper; Jenny Ooi initiated the project, performed the biochemistry and the initial MeCP2 fractionation into multiple complexes; Peter Yau performed the MS and identifications; Peter Jones conceived the project, funded the project, performed the biochemistry and wrote the paper.

ACKNOWLEDGEMENTS

We greatly appreciate the gift of HT-22 cells from Dr Stephanie Ceman. We thank Dr Ann Cheever and Dr Brian Imai for technical support, and Dr Takako I. Jones for help with the manuscript.

FUNDING

This work was supported by the National Institutes of Health, National Institute of Child Health and Human Development [grant number 5K22HD001338 (to P.L.J.)], and start-up funds from the School of Molecular and Cellular Biology and Department of Cell and Developmental Biology, University of Illinois at Urbana-Champaign (to P.L.J.).

REFERENCES

1 Meehan, R. R., Lewis, J. D. and Bird, A. P. (1992) Characterization of MeCP2, a vertebrate DNA binding protein with affinity for methylated DNA. Nucleic Acids Res. 20, 5085–5092
2 Hendrich, B. and Bird, A. (1998) Identification and characterization of a family of mammalian methyl-CpG binding proteins. Mol. Cell Biol. 18, 6538–6547
3 Jones, P. L., Veenstra, G. J., Wade, P. A., Vermaak, D., Kass, S. U., Landsberger, N., Strouboulis, J. and Wolffe, A. P. (1998) Methylated DNA and MeCP2 recruit histone deacetylase to repress transcription. Nat. Genet. 19, 187–191
4 Nan, X., Campoy, F. J. and Bird, A. (1997) MeCP2 is a transcriptional repressor with abundant binding sites in genomic chromatin. Cell 88, 471–481
5 Nan, X., Ng, H. H., Johnson, C. A., Laherty, C. D., Turner, B. M., Eisenman, R. N. and Bird, A. (1998) Transcriptional repression by the methyl-CpG-binding protein MeCP2 involves a histone deacetylase complex. Nature 393, 386–389
6 Amir, R. E., Van Den Veyver, I. B., Wan, M., Tran, C. Q., Francke, U. and Zoghbi, H. Y. (1999) Rett syndrome is caused by mutations in X-linked MECP2, encoding methyl-CpG-binding protein 2. Nat. Genet. 23, 185–188
7 Chahrour, M. and Zoghbi, H. Y. (2007) The story of Rett syndrome: from clinic to neurobiology. Neuron 56, 422–437
8 Rett, A. (1966) On an unusual brain atrophy syndrome in hyperammonemia in childhood. Wien Med. Wochenschr. 116, 723–726
9 Hagberg, B., Aicardi, J., Dias, K. and Ramos, O. (1983) A progressive syndrome of autism, dementia, ataxia, and loss of purposeful hand use in girls: Rett's syndrome: report of 35 cases. Ann. Neurol. 14, 471–479
10 Ylisaukko-Oja, T., Rehnstrom, K., Vanhala, R., Kempas, E., von Koskull, H., Tengstrom, C., Mustonen, A., Ounap, K., Lahdetie, J. and Jarvela, I. (2005) MECP2 mutation analysis in patients with mental retardation. Am. J. Med. Genet. A 132A, 121–124
11 Zoghbi, H. Y. (2005) MeCP2 dysfunction in humans and mice. J. Child Neurol. 20, 736–740
12 Carney, R. M., Wolpert, C. M., Ravan, S. A., Shahbazian, M., Ashley-Koch, A., Cuccaro, M. L., Vance, J. M. and Pericak-Vance, M. A. (2003) Identification of MeCP2 mutations in a series of females with autistic disorder. Pediatr. Neurol. 28, 205–211
13 Lam, C. W., Yeung, W. L., Ko, C. H., Poon, P. M., Tong, S. F., Chan, K. Y., Lo, I. F., Chan, L. Y., Hui, J. and Wong, V. (2000) Spectrum of mutations in the MECP2 gene in patients with infantile autism and Rett syndrome. J. Med. Genet. 37, E41
14 Watson, P., Black, G., Ramsden, S., Barrow, M., Super, M., Kerr, B. and Clayton-Smith, J. (2001) Angelman syndrome phenotype associated with mutations in MECP2, a gene encoding a methyl CpG binding protein. J. Med. Genet. 38, 224–228

15 Lunyak, V. V., Burgess, R., Prefontaine, G. G., Nelson, C., Sze, S. H., Chenoweth, J., Schwartz, P., Pevzner, P. A., Glass, C., Mandel, G. and Rosenfeld, M. G. (2002) Co-repressor-dependent silencing of chromosomal regions encoding neuronal genes. Science 298, 1747–1752
16 Kokura, K., Kaul, S. C., Wadhwa, R., Nomura, T., Khan, M. M., Shinagawa, T., Yasukawa, T., Colmenares, C. and Ishii, S. (2001) The Ski protein family is required for MeCP2-mediated transcriptional repression. J. Biol. Chem. 276, 34115–34121
17 Harikrishnan, K. N., Chow, M. Z., Baker, E. K., Pal, S., Bassal, S., Brasacchio, D., Wang, L., Craig, J. M., Jones, P. L., Sif, S. and El-Osta, A. (2005) Brahma links the SWI/SNF chromatin-remodeling complex with MeCP2-dependent transcriptional silencing. Nat. Genet. 37, 254–264
18 Agarwal, N., Hardt, T., Brero, A., Nowak, D., Rothbauer, U., Becker, A., Leonhardt, H. and Cardoso, M. C. (2007) MeCP2 interacts with HP1 and modulates its heterochromatin association during myogenic differentiation. Nucleic Acids Res. 35, 5402–5408
19 Klose, R. J. and Bird, A. P. (2004) MeCP2 behaves as an elongated monomer that does not stably associate with the Sin3a chromatin remodeling complex. J. Biol. Chem. 279, 46490–46496
20 Yasui, D. H., Peddada, S., Bieda, M. C., Vallero, R. O., Hogart, A., Nagarajan, R. P., Thatcher, K. N., Farnham, P. J. and Lasalle, J. M. (2007) Integrated epigenomic analyses of neuronal MeCP2 reveal a role for long-range interaction with active genes. Proc. Natl. Acad. Sci. U.S.A. 104, 19416–19421
21 Chahrour, M., Jung, S. Y., Shaw, C., Zhou, X., Wong, S. T., Qin, J. and Zoghbi, H. Y. (2008) MeCP2, a key contributor to neurological disease, activates and represses transcription. Science 320, 1224–1229
22 Skene, P. J., Illingworth, R. S., Webb, S., Kerr, A. R., James, K. D., Turner, D. J., Andrews, R. and Bird, A. P. (2010) Neuronal MeCP2 is expressed at near histone-octamer levels and globally alters the chromatin state. Mol. Cell 37, 457–468
23 Young, J. I., Hong, E. P., Castle, J. C., Crespo-Barreto, J., Bowman, A. B., Rose, M. F., Kang, D., Richman, R., Johnson, J. M., Berget, S. and Zoghbi, H. Y. (2005) Regulation of RNA splicing by the methylation-dependent transcriptional repressor methyl-CpG binding protein 2. Proc. Natl. Acad. Sci. U.S.A. 102, 17551–17558
24 Shahbazian, M. D., Antalffy, B., Armstrong, D. L. and Zoghbi, H. Y. (2002) Insight into Rett syndrome: MeCP2 levels display tissue- and cell-specific differences and correlate with neuronal maturation. Hum. Mol. Genet. 11, 115–124
25 Zoghbi, H. Y. (2003) Postnatal neurodevelopmental disorders: meeting at the synapse? Science 302, 826–830
26 Kishi, N. and Macklis, J. D. (2004) MECP2 is progressively expressed in post-migratory neurons and is involved in neuronal maturation rather than cell fate decisions. Mol. Cell Neurosci. 27, 306–321
27 Guy, J., Hendrich, B., Holmes, M., Martin, J. E. and Bird, A. (2001) A mouse Mecp2-null mutation causes neurological symptoms that mimic Rett syndrome. Nat. Genet. 27, 322–326
28 Chen, R. Z., Akbarian, S., Tudor, M. and Jaenisch, R. (2001) Deficiency of methyl-CpG binding protein-2 in CNS neurons results in a Rett-like phenotype in mice. Nat. Genet. 27, 327–331
29 Luikenhuis, S., Giacometti, E., Beard, C. F. and Jaenisch, R. (2004) Expression of MeCP2 in postmitotic neurons rescues Rett syndrome in mice. Proc. Natl. Acad. Sci. U.S.A. 101, 6033–6038
30 Ballas, N., Lioy, D. T., Grunseich, C. and Mandel, G. (2009) Non-cell autonomous influence of MeCP2-deficient glia on neuronal dendritic morphology. Nat. Neurosci. 12, 311–317
31 Wang, A., Forman-Kay, J., Luo, Y., Luo, M., Chow, Y. H., Plumb, J., Friesen, J. D., Tsui, L. C., Heng, H. H., Woolford, Jr, J. L. and Hu, J. (1997) Identification and characterization of human genes encoding Hprp3p and Hprp4p, interacting components of the spliceosome. Hum. Mol. Genet. 6, 2117–2126
32 Scanlan, M. J., Chen, Y. T., Williamson, B., Gure, A. O., Stockert, E., Gordan, J. D., Tureci, O., Sahin, U., Pfreundschuh, M. and Old, L. J. (1998) Characterization of human colon cancer antigens recognized by autologous antibodies. Int. J. Cancer 76, 652–658
33 Bi, X., Jones, T., Abbasi, F., Lee, H., Stultz, B., Hursh, D. A. and Mortin, M. A. (2005) *Drosophila* caliban, a nuclear export mediator, can function as a tumor suppressor in human lung cancer cells. Oncogene 24, 8229–8239
34 Lewis, J. D., Meehan, R. R., Henzel, W. J., Maurer-Fogy, I., Jeppesen, P., Klein, F. and Bird, A. (1992) Purification, sequence, and cellular localization of a novel chromosomal protein that binds to methylated DNA. Cell 69, 905–914
35 Matzat, L. H., Berberoglu, S. and Levesque, L. (2008) Formation of a Tap/NXF1 homotypic complex is mediated through the amino-terminal domain of Tap and enhances interaction with nucleoporins. Mol. Biol. Cell 19, 327–338
36 Lin, C., Yang, L., Yang, J. J., Huang, Y. and Liu, Z. R. (2005) ATPase/helicase activities of p68 RNA helicase are required for pre-mRNA splicing but not for assembly of the spliceosome. Mol. Cell. Biol. 25, 7484–7493
37 Jeffery, L. and Nakielny, S. (2004) Components of the DNA methylation system of chromatin control are RNA-binding proteins. J. Biol. Chem. 279, 49479–49487
38 Hite, K. C., Adams, V. H. and Hansen, J. C. (2009) Recent advances in MeCP2 structure and function. Biochem. Cell Biol. 87, 219–227
39 Neul, J. L., Fang, P., Barrish, J., Lane, J., Caeg, E. B., Smith, E. O., Zoghbi, H., Percy, A. and Glaze, D. G. (2008) Specific mutations in methyl-CpG-binding protein 2 confer different severity in Rett syndrome. Neurology 70, 1313–1321
40 Laurent, L., Wong, E., Li, G., Huynh, T., Tsirigos, A., Ong, C. T., Low, H. M., Kin Sung, K. W., Rigoutsos, I., Loring, J. and Wei, C. L. (2010) Dynamic changes in the human methylome during differentiation. Genome Res. 20, 320–331
41 Lauber, J., Plessel, G., Prehn, S., Will, C. L., Fabrizio, P., Groning, K., Lane, W. S. and Luhrmann, R. (1997) The human U4/U6 snRNP contains 60 and 90 kDa proteins that are structurally homologous to the yeast splicing factors Prp4p and Prp3p. RNA 3, 926–941
42 Stickeler, E., Fraser, S. D., Honig, A., Chen, A. L., Berget, S. M. and Cooper, T. A. (2001) The RNA binding protein YB-1 binds A/C-rich exon enhancers and stimulates splicing of the CD44 alternative exon v4. EMBO J. 20, 3821–3830
43 Shahbazian, M., Young, J., Yuva-Paylor, L., Spencer, C., Antalffy, B., Noebels, J., Armstrong, D., Paylor, R. and Zoghbi, H. (2002) Mice with truncated MeCP2 recapitulate many Rett syndrome features and display hyperacetylation of histone H3. Neuron 35, 243–254
44 Carbonnelle, D., Jacquot, C., Lanco, X., Le Dez, G., Tomasoni, C., Briand, G., Tsotinis, A., Calogeropoulou, T. and Roussakis, C. (2001) Up-regulation of a novel mRNA (NY-CO-1) involved in the methyl 4-methoxy-3-(3-methyl-2-butenoyl) benzoate (VT1)-induced proliferation arrest of a non-small-cell lung carcinoma cell line (NSCLC-N6). Int. J. Cancer 92, 388–397
45 Marchler-Bauer, A., Anderson, J. B., Chitsaz, F., Derbyshire, M. K., DeWeese-Scott, C., Fong, J. H., Geer, L. Y., Geer, R. C., Gonzales, N. R., Gwadz, M. et al. (2009) CDD: specific functional annotation with the Conserved Domain Database. Nucleic Acids Res. 37, D205–D210
46 Miyake, K. and Nagai, K. (2007) Phosphorylation of methyl-CpG binding protein 2 (MeCP2) regulates the intracellular localization during neuronal cell differentiation. Neurochem Int. 50, 264–270

Received 1 November 2010; accepted 11 November 2010
Published as Immediate Publication 11 November 2010, doi 10.1042/BSR20100124

Biosci. Rep. (2011) / **31** / 333–343 (Printed in Great Britain) / doi 10.1042/BSR20100124

online data

Original Paper

SUPPLEMENTARY ONLINE DATA

A brain-derived MeCP2 complex supports a role for MeCP2 in RNA processing

Steven W. LONG*, Jenny Y. Y. OOI*, Peter M. YAU*† and Peter L. JONES*‡[1]

*Department of Cell and Developmental Biology, University of Illinois at Urbana-Champaign, B107 Chemical and Life Sciences Laboratory, 601 S. Goodwin Ave., Urbana, IL 61801, U.S.A., †The Carver Biotechnology Center, University of Illinois at Urbana-Champaign, Urbana, IL 61801, U.S.A., and ‡The Boston Biomedical Research Institute, 64 Grove St, Watertown, MA 02472, U.S.A.

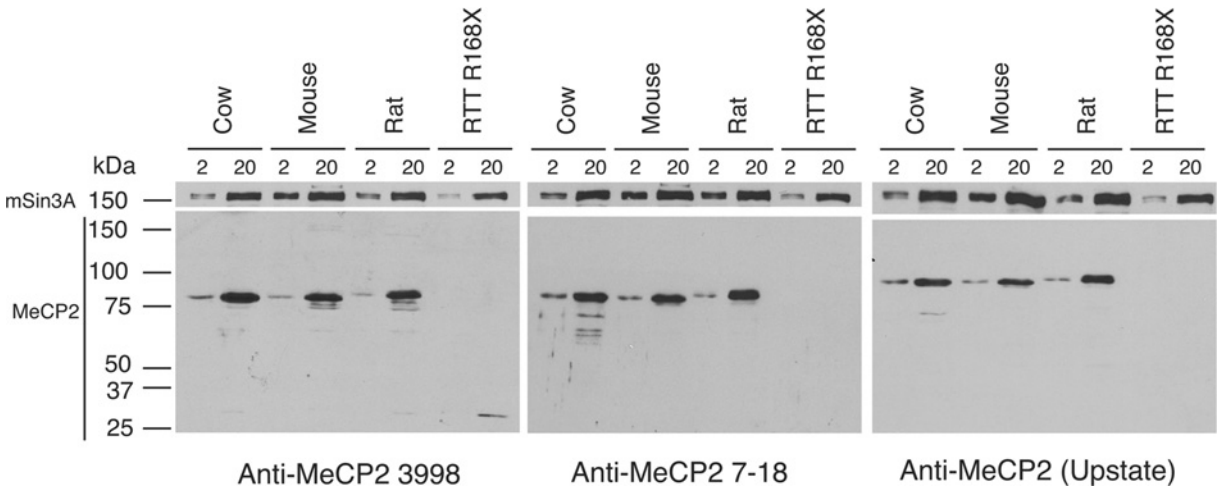

Figure S1 **Anti-MeCP2 antibodies react specifically with MeCP2 from multiple protein sources**
Antibodies against MeCP2 were used in Western blotting of brain nuclear extracts from cow, mouse and rat, and nuclear extracts from human lymphoblasts expressing the RTT R168X truncation to show their specificities. Anti-MeCP2 3998 (left-hand panel) [1] and anti-(MeCP2 7–18) (centre panel) antibodies generated by ourselves were compared with an anti-MeCP2 antibody purchased from Upstate Biotech (right-hand panel). All three antibodies react with a single polypeptide migrating at ~80 kDa, consistent with MeCP2s known migration on SDS/PAGE, in brain nuclear extracts (2 or 20 μg/lane) from cow, mouse and rat. These antibodies show no reactivity to any polypeptides in the human MeCP2 RTT R168X extracts by Western-blot analysis. These results confirm that the anti-MeCP2 7–17 antibody used in this study is specific for MeCP2. Load controls using an antibody for Sin3A [2] are shown above.

[1] To whom correspondence should be addressed (email pjones@bbri.org).

MeCP2 MonoQ flow-thru (QFT): Sequence coverage 41%

MVAGMLGLRKEKSEDQDLQGLKEKPLKFKKVKKDKKEDKEGKHEPLQPSAHH
SAEPAEAGKAETSESSGSAPAVPEASASPKQRRSIIRDRGPMYDDPTLPEGWTRK
LKQRKSGRSAGKYDVYLINPQGKAFRSKVELIAYFEKVGDTSLDPNDFDFTVTG
RGSPSRREQKPPKKPKSPKAPGTGRGRGRPKGSGTGRPKAAASEGVQVKRVLEK
SPGKLLVKMPFQASPGGKGEGGGATTSAQVMVIKRPGRKRKAEADPQAIPKKR
GRKPGSVVAAAAAEAKKKAVKESSIRSVQETVLPIKKRKTRETVSIEVKEVVKPL
LVSTLGEKSGKGLKTCKSPGRKSKESSPKGRSSSASSPPKKEHHHHHHHAESPKA
PMPLLPPPPPPEPQSSEDPISPPEPQDLSSSICKEEKMPRAGSLESDGCPKEPAKTQP
MVAAAATTTTTTTTTVAEKYKHRGEGERKDIVSSSMPRPNREEPVDSRTPVTER
VS

MeCP2 MonoQ bound 2 (QB2): Sequence coverage 23%

MVAGMLGLRKEKSEDQDLQGLKEKPLKFKKVKKDKKEDKEGKHEPLQPSAHH
SAEPAEAGKAETSESSGSAPAVPEASASPKQRRSIIRDRGPMYDDPTLPEGWTRK
LKQRKSGRSAGKYDVYLINPQGKAFRSKVELIAYFEKVGDTSLDPNDFDFTVTG
RGSPSRREQKPPKKPKSPKAPGTGRGRGRPKGSGTGRPKAAASEGVQVKRVLEK
SPGKLLVKMPFQASPGGKGEGGGATTSAQVMVIKRPGRKRKAEADPQAIPKKR
GRKPGSVVAAAAAEAKKKAVKESSIRSVQETVLPIKKRKTRETVSIEVKEVVKPL
LVSTLGEKSGKGLKTCKSPGRKSKESSPKGRSSSASSPPKKEHHHHHHHAESPKA
PMPLLPPPPPPEPQSSEDPISPPEPQDLSSSICKEEKMPRAGSLESDGCPKEPAKTQP
MVAAAATTTTTTTTTVAEKYKHRGEGERKDIVSSSMPRPNREEPVDSRTPVTER
VS

MeCP2 MonoQ bound 3 (QB3): Sequence coverage 33%

MVAGMLGLRKEKSEDQDLQGLKEKPLKFKKVKKDKKEDKEGKHEPLQPSAHH
SAEPAEAGKAETSESSGSAPAVPEASASPKQRRSIIRDRGPMYDDPTLPEGWTRK
LKQRKSGRSAGKYDVYLINPQGKAFRSKVELIAYFEKVGDTSLDPNDFDFTVTG
RGSPSRREQKPPKKPKSPKAPGTGRGRGRPKGSGTGRPKAAASEGVQVKRVLEK
SPGKLLVKMPFQASPGGKGEGGGATTSAQVMVIKRPGRKRKAEADPQAIPKKR
GRKPGSVVAAAAAEAKKKAVKESSIRSVQETVLPIKKRKTRETVSIEVKEVVKPL
LVSTLGEKSGKGLKTCKSPGRKSKESSPKGRSSSASSPPKKEHHHHHHHAESPKA
PMPLLPPPPPPEPQSSEDPISPPEPQDLSSSICKEEKMPRAGSLESDGCPKEPAKTQP
MVAAAATTTTTTTTTVAEKYKHRGEGERKDIVSSSMPRPNREEPVDSRTPVTER
VS

Figure S2 **MS MeCP2 peptide identifications**
MS identified peptides (in red) are shown in the predicted amino acid sequences for rat MeCP2 from the QF, QB2 and QB3 pools of MeCP2.

EIF2S1 [eukaryotic translation initiation factor 2, subunit 1] Sequence Coverage: 33%

MPGLSCRFYQHKFPEVEDVVMVNVRSIAEMGAYVSLLEYNNIEGMILLSELSRR
RIRSINKLIRIGRNECVVVIRVDKEKGYIDLSKRRVSPEEAIKCEDKFTKSKTVYSI
LRHVAEVLEYTKDEQLESLFQRTAWVFDDKYKRPGYGAYDAFKHAVSDPSILDS
LDLNEDEREVLINNINRRLTPQAVKIRADIEVACYGYEGIDAVKEALRAGLNCST
ETMPIKINLIAPPRYVMTTTTLERTEGLSVLNQAMAVIKEKIEEKRGVFNVQMEP
KVVTDTDETELARQLERLERENAEVDGDDDAEEMEAKAED

EIF2S2 [eukaryotic translation initiation factor 2, subunit 2] Sequence Coverage: 30%

MSGDEMIFDPTMSKKKKKKKKPFMLDEEGDAQTEETQPSETKEVEPEPAEEKDV
EADEEDSRKKDASDDLDDLNFFNQKKKKKTKKIFDIDEAEEAIKDVKIESDAQE
PAEPEDDLDIMLGNKKKKKKNVKFPDEDEILEKDEALEDEDSKKDDGISFSNQTG
PAWAGSERDYTYEELLNRVFNIMREKNPDMVAGEKRKFVMKPPQVVRVGTKK
TSFVNFTDICKLLHRQPKHLLAFLLAELGTSGSIDGNNQLVIKGRFQQKQIENVLR
RYIKEYVTCHTCRSPDTILQKDTRLYFLQCETCHSRCSVASIKTGFQAVTGKRAQ
LRAKAN

EIF2S3 [eukaryotic translation initiation factor 2, subunit 3] Sequence Coverage: 37%

MAGGEAGVTLGQPHLSRQDLATLDVTKLTPLSHEVISRQATINIGTIGHVAHGKS
TVVKAISGVHTVRFKNELERNITIKLGYANAKIYKLDDPSCPRPECYRSCGSSTPD
EFPTDIPGTKGNFKLVRHVSFVDCPGHDILMATMLNGAAVMDAALLLIAGNESC
PQPQTSEHLAAIEIMKLKHILILQNKIDLVKESQAKEQYEQILAFVQGTVAEGAPII
PISAQLKYNIEVVCEYIVKKIPVPPRDFTSEPRLIVIRSFDVNKPGCEVDDLKGGVA
GGSILKGVLKVGQEIEVRPGIVSKDSEGKLMCKPIFSKIVSLFAEHNDLQYAAPGG
LIGVGTKIDPTLCRADRMVGQVLGAVGALPEIFTELEISYFLLRRLLGVRTEGDKK
AAKVQKLSKNEVLMVNIGSLSTGGRVSAVKADLGKIVLTNPVCTEVGEKIALSR
RVEKHWRLIGWGQIRRGVTIKPTVDDD

Mecp2 [Methyl-CpG-binding protein 2] Sequence Coverage: 23%

MVAGMLGLRKEKSEDQDLQGLKEKPLKFKKVKKDKKEDKEGKHEPLQPSAHH
SAEPAEAGKAETSESSGSAPAVPEASASPKQRRSIIRDRGPMYDDPTLPEGWTRK
LKQRKSGRSAGKYDVYLINPQGKAFRSKVELIAYFEKVGDTSLDPNDFDFTVTG
RGSPSRREQKPPKKPKSPKAPGTGRGRGRPKGSGTGRPKAAASEGVQVKRVLEK
SPGKLLVKMPFQASPGGKGEGGGATTSAQVMVIKRPGRKRKAEADPQAIPKKR
GRKPGSVVAAAAAEAKKKAVKESSIRSVQETVLPIKKRKTRETVSIEVKEVVKPL
LVSTLGEKSGKGLKTCKSPGRKSKESSPKGRSSSASSPPKKEHHHHHHHAESPKA
PMPLLPPPPPPEPQSSEDPISPPEPQDLSSSICKEEKMPRAGSLESDGCPKEPAKTQP
MVAAAATTTTTTTTTVAEKYKHRGEGERKDIVSSSMPRPNREEPVDSRTPVTER
VS

PRPF3 [PRP3 pre-mRNA processing factor 3 homolog] Sequence Coverage: 9%

MALSKRELDELKPWIEKTVKRVLGFSEPTVVTAALNCVGKGMDKKKAADHLKP
FLDDSTLRFVDKLFEAVEEGRSSRHSKSSSDRSRKRELKEVFGDDSEISKESSGVK
KRRIPRFEEVEEEPEVIPGPPSESPGMLTKLQIKQMMEAATRQIEERKKQLSFISPP
APQPKTPSSSQPERLPIGNTIQPSQAATFMNDAIEKARKAAELQARIQAQLALKPG
LIGNANMVGLANLHAMGIAPPKVELKDQTKPTPLILDEQGRTVDATGKEVELTH
RMPTLKANIRAVKREQFKQQLKEKPSEDMESNTFFDPRVSIAPSQRQRRTFKFHD
KGKFEKIAQRLRTKAQLEKLQAEISQAARKTGIHTSTRLALIAPKKELKEGDIPEIE
WWDSYIIPNGFDLTEENPKREDYFGITNLVEHPAQLNPPVDNDTPVTLGVYLTKK
EQKKLRRQTRREAQKELQEKVRLGLTPPPEPKVRISNLMRVLGTEAVQDPTKVE
AHVRAQMAKRQKAHEEANAARKLTAEQRKVKKVKKLKEDISQGVHISVYRVR
NLSNPAKKFKIEANAGQLYLTGVVVLHKDVNVVVVEGGPKAQRKFKRLMLHRI
KWDEQTSNTKGDDDEESDEEAVKKTNKCVLVWEGTAKDRSFGEMKFKQCPTE
NMAREHFKKHGAEHYWDLALSESVLESTD

ABCF1 [PREDICTED: similar to ATP-binding cassette sub-family F member 1 (ATP-binding cassette 50)]
Sequence Coverage: 32%

MPKGPKQQPPEPEWIGDGEGTSPADKVVKKGKKDKKTKKTFFEELAVEDKQAG
EEEKLQKEKEQQQQQQQQKKKRDTRKGRRKKDVDDDDDGDERVLMERLKQLS
VPASDEEDEVPVPVPRGRKKAKGGNVFEALIQDESEEEKEEEEEKPVLKPAKPEK
NRINKAVAEEPPGLRNKKGKEEKSKGKAKNKPSATDSEGEDDEDMTKEKEPPRP
GKDKDKKGAEQGSEEEKEEKEGEVKANDPYAHLSKKEKKKLKKQMDYERQVE
SLKAANAAENDFSVSQAEVSSRQAMLENASDIKLEKFSISAHGKELFVNADLYIV
AGRRYGLVGPNGKGKTTLLKHIANRALSIPPNIDVLLCEQEVVADETPAVQAVLR
ADTKRLRLLEEEKRLQGQLEQGDDTAAEKLEKVYEELRATGAAAAEAKARRIL
AGLGFDPEMQNRPTQKFSGGWRMRVSLARALFMEPTLLMLDEPTNHLDLNAVI
WLNNYLQGWRKTLLIVSHDQGFLDDVCTDIIHLDTQRLHYYRGNYMTFKKMYQ
QKQKELLKQYEKQEKKLKELKAGGKSTKQAEKQTKEVLTRKQQKCRRKNQDE
ESQDPPELLKRPREYTVRFTFPDPPPLSPPVLGLHGVTFGYEGQKPLFKNLDFGID
MDSRICIVGPNGVGKSTLLLLLTGKLTPTNGEMRKNHRLKIGFFNQQYAEQLHM
EETPTEYLQRGFNLPYQDARKCLGRFGLESHAHTIQICKLSGGQKARVVFAELAC
REPDVLILDEPTNNLDIESIDALGEAINEYKGAVIVVSHDARLITETNCQLWVVEE
QSVSQIDGDFDDYKREVLEALGEVMVNRPRD

SDCCA1 [similar to serologically defined colon cancer antigen 1]
Sequence Coverage: 3%

MKTRFSTVDLRAVLAELNANLLGMRVNNVYDVDNKTYLIRLQKPDFKATLLLE
SGIRIYTTEFEWPKNMMPSSFAMKCRKHLKSRRLVSAKQLGVDRIVDFQFGSDE
AAYHLIIELYDRGNIVLTDYEYLILNILRFRTDEADDVKFAVRERYPIDHARAAEP
LLTLERLTEVIARAPRGELLKRVLNLLLPYGPALIEHCLIENGFSGNVKVDEKLES
KDIEKILVCVQRAEDYLEKTANFNGKGYIIQKREVKPSLDANKPAEDILMYEEFH
PFLFSOHLOCPYIEFESFDKEKOALKKLDNVXKDHENRLEALOOAOEIDKLKGEL
IEMNLQIVDRAIQVVRSALANQIDWTEIGVIVKEAQAQGDHVASAIKELKLQTNH
ITMLLRNPYLLSEEEDGDGDGSIENSDAEAPKGKKKAKEQAAAEASEGQAAACR
CGPQPVSLCQCQKVLXSXEVCCXKTTENCRSCXEGIQISREENKANLKRSTNSYF
YPKSKESVLVXEISVVYXFRELSHYRWSRSATEXDYCEKILNTRRHLCACXSSWS
YQLCNXESNRRSHPSSDFDXSRHNGTLLQRGLGCPCYHECLVGAPSSGIXNSTDR
RVLNNWKLHDKRKKEFPSSFIPNDGVXLPFXGRXVLCLETSRXTKRQSAGXRHE
NIDKLHKXTHVRRNGTARRGRQQXRRDRGVMWNHGRSGTQDSGXSRGHCCSQ
WKRGTELXRWRSHQNSHERXRAHWXGEGRGGRISXHHHXLVPSSVPKAPTETD
SKRRIFXFKXQXITEPKTFVSQGEKRNEKEKAPMXLRGFRSDRRKGQRKRKCCA
QXSXPEHKQKCGSWTANEKRPEEXNEKNEGKIQRPGXXRSXTYYEIVGICRFKQ
RRKGEERKERKNKRXTREKKPTETQRWTAGFRCCXRNPVPSGVDSXLTRLCCG
XATXXQGRTXSGSAGKXGKSIXLFDRATTSXRCTNVCYSNMCSLHHHDKLXIQS
ETYSWSSEKGKSCKDSLEQFHALQRSNSKRKRLIPKCEGHRFTKKHSRESESVCP
QSSARKKKI

Figure S3 **MS identifications of MeCP2 co-purifying peptides**
MS identified peptides (in red) for the MeCP2 co-purifying polypeptides from the QB2 pool of MeCP2.

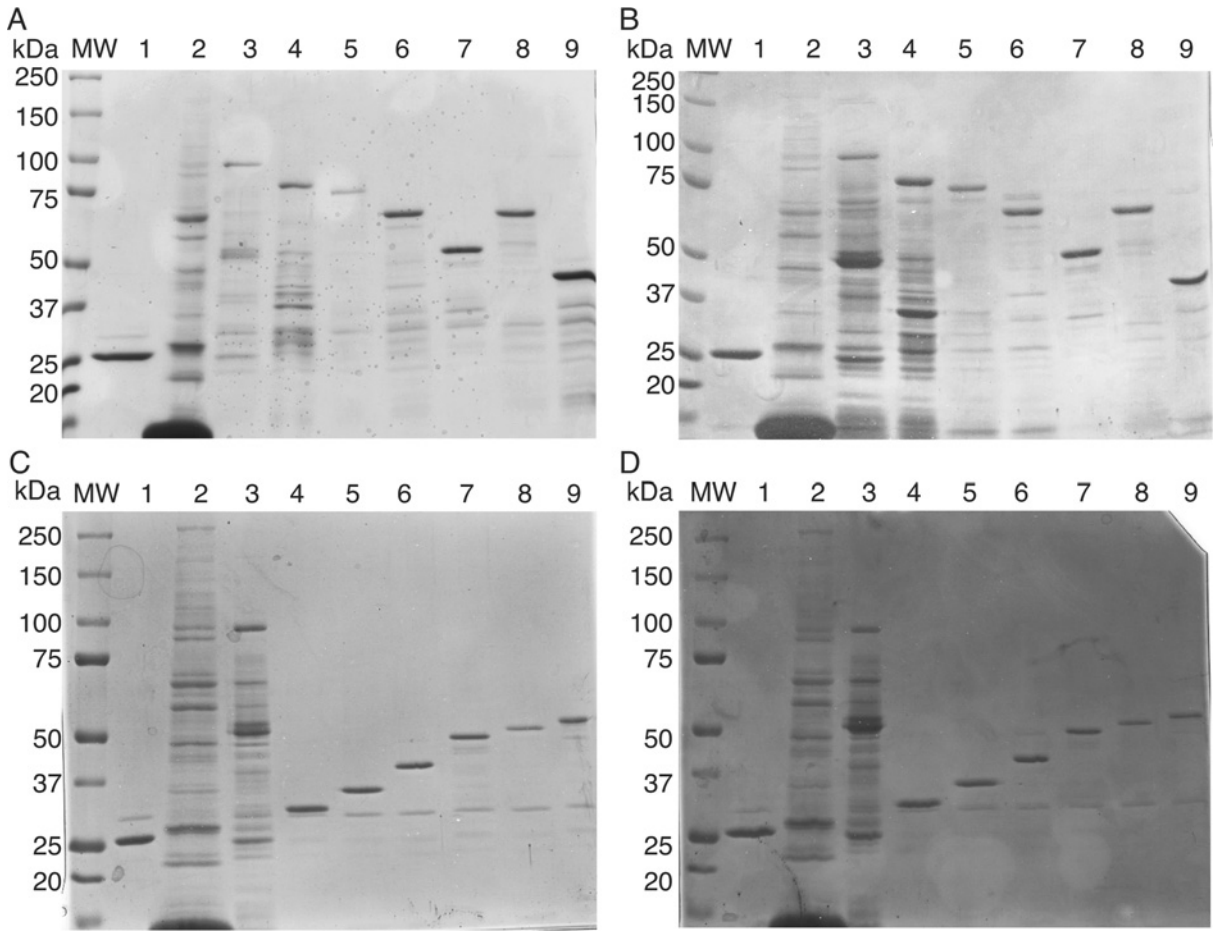

Figure S4 **GST input control gels**

Coomassie Brilliant Blue stained SDS/PAGE gels from GST pull-down experiments show equivalent levels of GST-fusion proteins in each pull-down reaction. (A) GST-fusion proteins from Figure 4(C) of the main paper, Prpf3. (B) GST-fusion proteins from Figure 4(C) of the main paper, Sdccag1. (C) GST-fusion proteins from Figure 6(A) of the main paper, Prpf3. (D) GST-fusion proteins from Figure 6(A) of the main paper, Sdccag1.

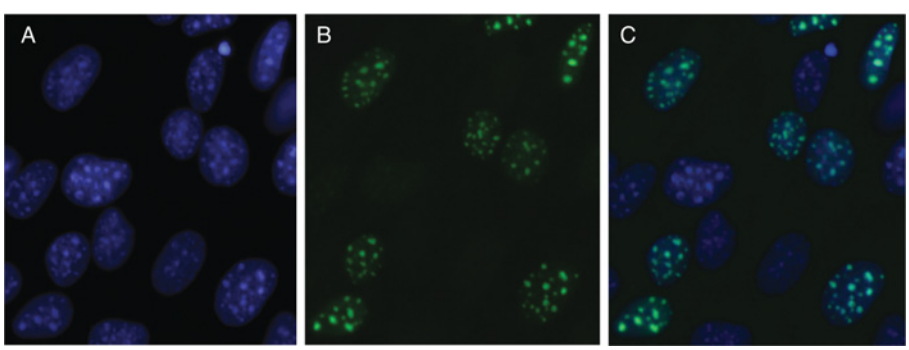

Figure S5 **Characterization of HA–MeCP2 expressing HT22 cells**

HT22 hippocampal neuronal cells stably transected with HA–MeCP2, visualized by (A) DAPI (4′,6-diamidino-2-phenylidole) staining and (B) indirect immunofluorescence for HA–MeCP2 with (C) images merged, show HA–MeCP2 localizes to heterochromatic foci.

Table 1 PCR and RT–PCR oligonucleotide primers

Primer	Plasmid construct	Sequence (5′→3′)
1	pGEM ratAbcf1	ATGCCGAAGGGTCCCAAGCAGC
2	pGEM ratAbcf1	TCAATCCCGAGGTCGGTTGAC
3	pGEM ratEif2s1	ATGCCGGGTCTAAGTTGTAGATTTTATCAACAC
4	pGEM ratEif2s1	TTAATCTTCAGCTTTGGCTTCCATTTCTTCTGC
5	pGEM ratEif2s2	ATGTCCGGGGACGAGATGATTTTTGATCCTAC
6	pGEM ratEif2s2	TTAGTTAGCTTTGGCACGGAGCTG
7	pGEM ratEif2s3	ATGGCTGGGGGTGAGGCTG
8	pGEM ratEif2s3	TCAGTCATCATCTACAGTCGGCTTAATG
9	pGEM ratMeCP2	ATGGTAGCTGGGATGTTAGGGC
10	pGEM ratMeCP2	TCAGCTAACTCTCTCGGTCACG
11	pGEM ratPrpf3	ATGGCACTGTCTAAGCGGGAACTGGATG
12	pGEM ratPrpf3	CTACAGAGAACATGGCGCGTGA
13	pGEM ratSdccag1	ATGAAGACCCGCTTCAGCACTGTTGAC
14	pGEM ratSdccag1	CTATTTTCTTTTTACGTGCAGAAGATTGGG
15	pGEM human Prpf3	ATGGCACTGTCAAAGAGGGAGC
16	pGEM human Prpf3	TCAATCAGTGGACTCTAAC
17	pCDNA3.1 ratAbcf1	GCGGCCGCATGCCGAAGGGTCC
18	pCDNA3.1 ratAbcf1	CGCTCGAGTCAATCCCGAGGTCGG
19	pCDNA3.1 ratEif2s1	GCGGCCGCATGCCGGGTCTAAG
20	pCDNA3.1 ratEif2s1	CGCTCGAGTTAATCTTCAGCTTTGGCTTC
21	pCDNA3.1 ratEif2s2	GCGGCCGCATGTCCGGGGAC
22	pCDNA3.1 ratEif2s2	CGCTCGAGTTAGTTAGCTTTGGCACG
23	pCDNA3.1 ratEif2s3	GCGGCCGCATGGCTGGGGGTG
24	pCDNA3.1 ratEif2s3	CGCTCGAGTCAGTCATCATCTACAGTCG
25	pCDNA3.1 ratMeCP2	GCGGCCGCATGGTAGCTGGGATG
26	pCDNA3.1 ratMeCP2	CGCTCGAGTCAGCTAACTCTCTCGGTC
27	pCDNA3.1HA humanMeCP2	GCGGCCGCATGGTAGCTGGGATG
28	pCNA3.1HA humanMeCP2	CGCTCGAGTCAGCTAACTCTCTCGGTC
29	pCDNA3.1 ratPrpf3	GCGGCCGCATGGCACTGTCTAAGC
30	pCDNA3.1 ratPrpf3	CGCTCGAGTCACGCGCCATGTTCTC
31	pCDNA3.1 ratSdccag1	GCGGCCGCATGAAGAGCCGCT
32	pCDNA3.1 ratSdccag1	CGCTCGAGCTATTTCCTTTTTACGTTCAGAAG
33	pCDNA3.1 humanPrpf3	AGAATTCATGGCACTGTCAAAGAG
34	pCDNA3.1 humanPrpf3	CTCGAGTCAATCAGTGGACTCTAAC
35	pGEX5X ratPrpf3	AGAATTCATGGCACTGTCTAAGC
36	pGEX5X ratPrpf3	CTCGAGTCACGCGCCATGTTCTC
37	pGEX5X MeCP2 d1	AGAATTCGCCTCCCCCAAACAG
38	pGEX5X MeCP2 d1	CTCGAGTCAGCTAACTCTCTCGG
39	pGEX5X MeCP2 d2	AGAATTCAAGCAAAGGAAATCTGGC
40	pGEX5X MeCP2 d2	CTCGAGTCAGCTAACTCTCTCGG
41	pGEX5X MeCP2 d3	AGAATTCGGCACCACGAGACC
42	pGEX5X MeCP2 d3	CTCGAGTCAGCTAACTCTCTCGG
43	pGEX5X MeCP2 d4	AGAATTCACGGTCAGCATCGAG
44	pGEX5X MeCP2 d4	CTCGAGTCAGCTAACTCTCTCGG
45	pGEX5X MeCP2 d5	AGAATTCATGGTAGCTGGGATGTTAG
46	pGEX5X MeCP2 d5	CTCGAGGGTCTTGCGCTTCTTG
47	pGEX5X MeCP2 d6	AGAATTCGGCACCACGAGACC
48	pGEX5X MeCP2 d6	CTCGAGACCGAGGGTGGACAC
49	RT–PCR mouseFRG1 5′	AATTGCCCTGAAGTCTGGCTATGG
50	RT–PCR mouseFRG1 3′	CTTTCAATTTGGCTCTCCTGTCCAG

Table 2 Continued

Primer	Plasmid construct	Sequence (5′→3′)
51	RT–PCR mouseCDK10 5′	GGCCAGGGATACCCAGACAG
52	RT–PCR mouseCDK10 3′	CCTCCGAGAAGGGTGTTGGC
53	RT–PCR mouseCasc3 5′	CTACAGTGAAGAGGAGAATTCCAAGGTG
54	RT–PCR mouseCasc3 3′	GATCCTCATCGTCATCCAAGTGC
55	pGEX5X MeCP2 S49X	AGAATTCGCCTCCCCCAAACAG
56	pGEX5X MeCP2 S49X	ACTCGAGTCATGGCTGCACGGGC
57	pGEX5X MeCP2 S68X	AGAATTCGCCTCCCCCAAACAG
58	pGEX5X MeCP2 S68X	ACTCGAGTCACCCTTCTGATGTCTC
59	pGEX5X MeCP2 W104X	AGAATTCGCCTCCCCCAAACAG
60	pGEX5X MeCP2 W104X	ACTCGAGTCAGCCTTCAGGCAGG
61	pGEX5X MeCP2 Y141X	AGAATTCGCCTCCCCCAAACAG
62	pGEX5X MeCP2 Y141X	ACTCGAGTCACGCAATCAACTCC
63	pGEX5X MeCP2 R168X	AGAATTCGCCTCCCCCAAACAG
64	pGEX5X MeCP2 R168X	ACTCGAGTCATCATCTCGCCGGGAGGG
65	pGEX5X MeCP2 S204X	AGAATTCGCCTCCCCCAAACAG
66	pGEX5X MeCP2 S204X	CTCGAGTCACGTGGCCGCCTTG
67	pGEX5X MeCP2 R106W	AGAATTCATGGTAGCTGGGATGTTAGGG
68	pGEX5X MeCP2 R106W	CTCGAGTCAGCTAACTCTCTCGGTC
69	pGEX5X MeCP2 F155S	AGAATTCATGGTAGCTGGGATGTTAGGG
70	pGEX5X MeCP2 F155S	CTCGAGTCAGCTAACTCTCTCGGTC
71	pGEX5X MeCP2 R294X	AGAATTCATGGTAGCTGGGATGTTAGGG
72	pGEX5X MeCP2 R294X	CTCGAGTCATCGGATAGAAGACTCCTTC
73	pGEX5X MeCP2 F155S/R294X	AGAATTCATGGTAGCTGGGATGTTAGGG
74	pGEX5X MeCP2 F155S/R294X	CTCGAGTCATCGGATAGAAGACTCCTTC
75	pGEX5X MeCP2 H370X	AGAATTCATGGTAGCTGGGATGTTAGGG
76	pGEX5X MeCP2 H370X	CTCGAGTCAGTGATGGTGGTGGTGC
77	pGEX5X MeCP2 E397X	AGAATTCATGGTAGCTGGGATGTTAGGG
78	pGEX5X MeCP2 E397X	CTCGAGTCACTCGGAGCTCTCGG
79	pGEX5X MeCP2 R453X	AGAATTCATGGTAGCTGGGATGTTAGGG
80	pGEX5X MeCP2 R453X	CTCGAGTCATCGGTGTTTGTACTTTTCTG

REFERENCES

1 Harikrishnan, K. N., Chow, M. Z., Baker, E. K., Pal, S., Bassal, S., Brasacchio, D., Wang, L., Craig, J. M., Jones, P. L., Sif, S. and El-Osta, A. (2005) Brahma links the SWI/SNF chromatin-remodeling complex with MeCP2-dependent transcriptional silencing. Nat. Genet. 37, 254–264

2 Jones, P. L., Veenstra, G. J., Wade, P. A., Vermaak, D., Kass, S. U., Landsberger, N., Strouboulis, J. and Wolffe, A. P. (1998) Methylated DNA and MeCP2 recruit histone deacetylase to repress transcription. Nat. Genet. 19, 187–191

Received 1 November 2010; accepted 11 November 2010
Published as Immediate Publication 11 November 2010, doi 10.1042/BSR20100124